Please cite this article in press as: Panchal et al., Reduced Levels of Protein Tyrosine Phosphatase CD45 Protect Mice from the Lethal Effects of Ebola Virus Infection, Cell Host & Microbe (2009), doi:10.1016/j.chom.2009.07.003

Cell Host & Microbe
Article

Reduced Levels of Protein Tyrosine Phosphatase CD45 Protect Mice from the Lethal Effects of Ebola Virus Infection

Rekha G. Panchal,[1,*] Steven B. Bradfute,[1] Brian D. Peyser,[1] Kelly L. Warfield,[1] Gordon Ruthel,[1] Douglas Lane,[2] Tara A. Kenny,[2] Arthur O. Anderson,[1] William C. Raschke,[3,4] and Sina Bavari[1,*]
[1]United States Army Medical Research Institute of Infectious Diseases, 1425 Porter Street, Fort Detrick, Frederick, MD 21702-5011, USA
[2]Target Structure Based Drug Discovery Group, SAIC-Frederick, Inc., NCI-Frederick, Frederick, Maryland, 21702-1201, USA
[3]Sidney Kimmel Cancer Center, 10905 Road to the Cure, San Diego, CA 92121, USA
[4]Virogenics, Inc., P.O. Box 2702, Del Mar, CA 92104, USA
*Correspondence: rekha.panchal@amedd.army.mil (R.G.P.), sina.bavari@amedd.army.mil (S.B.)
DOI 10.1016/j.chom.2009.07.003

SUMMARY

Ebola virus (EBOV) infection of humans is a lethal but accidental dead-end event. Understanding resistance to EBOV in other species may help establish the basis of susceptibility differences among its hosts. Although rodents are resistant to EBOV, a murine-adapted variant is lethal when injected intraperitoneally into mice. We find that mice expressing reduced levels of the tyrosine phosphatase CD45 are protected against EBOV, whereas wild-type, CD45-deficient, or enzymatically inactive CD45-expressing mice succumbed to infection. Protection was dependent on CD8$^+$ T cells and interferon γ. Reduced CD45-expressing mice retained greater control of gene expression and immune cell proliferation following EBOV infection, which contributed to reduced apoptosis, enhanced viral clearance, and increased protection against the virus. Together, these findings suggest that host susceptibility to EBOV is dependent on the delicate balance of immune homeostasis, which, as demonstrated here, can be determined by the levels of a single regulator.

INTRODUCTION

Ebola virus (EBOV), a member of the family *Filoviridae*, is a single-stranded, negative-sense RNA virus that can cause acute hemorrhagic fever and rapid death within 7–14 days following infection in humans and nonhuman primates (Hoenen et al., 2006). There are at least five different species of EBOV—Zaire, Sudan, Ivory Coast, Reston, and the recently identified Bundibugyo virus (Towner et al., 2008)—having different patterns of pathogenicity in nonhuman primates and man (for example, EBOV-Reston causes no disease in man, whereas EBOV-Zaire is highly lethal). Several animal models have been developed to study the pathogenesis of filoviruses, including mouse, guinea pig, hamster and nonhuman primate models (Bowen et al., 1978; Bray et al., 1998; Connolly et al., 1999; Ryabchikova et al., 1996). Adult mice are resistant to naturally occurring isolates of EBOV. However, a mouse-adapted variant of the Ebola Zaire virus is lethal when injected via the intraperitoneal route of infection, but not other routes (Bray et al., 1998). The natural reservoir of EBOV is unknown, but it is clear that the infection of nonhuman primates and humans is an accidental dead-end event and that none of the physiologic abnormalities that occur during its course are the result of evolutionary adaptation of the virus to humans (Warfield et al., 2009). The resistance of other species such as rodents may allow for determination of the differences in the susceptibility between different accidental hosts. The interaction between the virus and immune cells plays a critical role in the pathogenesis of this disease. During the early stage of infection, the virus infects cells of the monocytic lineage, including dendritic cells (DCs), monocytes, and macrophages, whereupon these cells die or become nonfunctional and lose their ability to stimulate antigen-specific T cells (Mohamadzadeh et al., 2007). As the disease progresses, there is increased release of proinflammatory cytokines, lymphocyte apoptosis, and spread of the virus to nonlymphocytic cell types such as hepatocytes (Mohamadzadeh, 2009; Mohamadzadeh et al., 2007). Thus, multiple mechanisms have been shown to contribute to EBOV pathogenesis.

Protein tyrosine phosphatases (PTPs) are critical regulators of signal transduction and include a set of 107 genes within the human genome (Alonso et al., 2004). Among these is CD45, an abundant protein expressed in nucleated cells of hematopoietic origin (Thomas, 1989). The primary role of CD45 is regulation of antigen-receptor signaling of T and B cells via dephosphorylation of the Src family kinases (SFKs) (Alexander, 2000; Hermiston et al., 2003; Thomas and Brown, 1999). CD45 can act both as a positive and negative regulator of SFKs, depending on the nature of the stimulus, the cell type involved, and the developmental stage of the cells (Alexander, 2000; Hermiston et al., 2003; Thomas and Brown, 1999). In addition to its role in regulating intracellular signaling, CD45 is thought to play a role in mediating cell-cell contact by modulating integrin-mediated adhesion (Roach et al., 1997). Thus, CD45 is a pleiotropic mediator of lymphocyte function.

We recently observed that mice expressing intermediate levels of CD45 were protected against the highly virulent Ames strain of *B. anthracis*, a gram-positive spore-forming bacterium (Panchal et al., 2009). To explore the beneficial effects of

Please cite this article in press as: Panchal et al., Reduced Levels of Protein Tyrosine Phosphatase CD45 Protect Mice from the Lethal Effects of Ebola Virus Infection, Cell Host & Microbe (2009), doi:10.1016/j.chom.2009.07.003

Table 1. Genotype of the Transgenic and Heterozygous Mice and Corresponding Percentage of CD45 Expression

Genotype	% CD45 Expression[b]	Text Designation
$KO^{-/-}$	0	$CD45^{0\%}$
$B^{+/-}$	11	$CD45^{11\%}$
$B^{+/+}$	22	$CD45^{22\%}$
$F^{+/-}$	36	$CD45^{36\%}$
$het^{+/-}$	62	$CD45^{62\%}$
$F^{+/-}$ $E^{+/-}$	77	$CD45^{77\%}$
$WT^{+/+}$	100	$CD45^{100\%}$
$CSV10^{+/-}$[a]	62	$CSV10^{+/-}$
$CSV10^{+/+}$[a]	100	$CSV10^{+/+}$

E indicates the endogenous allele of normal mice.
[a] Cysteine-to-serine point mutation (C817S) in founder mouse V10 inactivating the CD45 phosphatase activity.
[b] All expression levels represent means with variation of ± 3%.

modulating CD45 levels in other disease models and to investigate whether evolutionarily distinct pathogens share a convergent host pathway that could serve as a common therapeutic target, mice expressing differential levels of CD45 were challenged with EBOV. In this study, we show that reduced CD45 expression levels protect mice from the lethal effects of EBOV infection. Mechanistic studies of mice challenged with EBOV revealed that reduced CD45 expression levels retained the ability to properly regulate early gene expression and inflammation, as well as generated a robust protective immunity response. All of these concerted changes contributed to reduced apoptosis and rapid viral clearance, leading to the survival of the mice.

RESULTS

Mice Expressing Reduced CD45 Levels Survive Ebola Challenge

The pathogenesis of the mouse-adapted EBOV-Zaire infections in mice largely resembles that in guinea pigs and nonhuman primates (Bradfute et al., 2007, 2008; Bray et al., 1998), although subtle differences in coagulopathy have also been observed (Gibb et al., 2001). Therefore, to explore the role of reduced CD45 expression in EBOV pathogenesis, we utilized mice engineered to express a range of CD45 levels (11%, 22%, 36%, 62%, and 77% of the wild-type level) and mice with a point mutation C817S, inactivating CD45 phosphatase activity but expressing 62% ($CSV10^{+/-}$) or 100% ($CSV10^{+/+}$) of the wild-type CD45 protein, were utilized (Table 1). These cell-surface CD45 expression levels were determined by flow cytometry using erythrocyte-depleted blood cells (Figure 1A) and based on comparison of mean fluorescence intensity with wild-type controls. The different mice groups were challenged with > 3000 LDB_{50B} of mouse-adapted EBOV. Mice expressing 11%–77% CD45 levels were protected from lethal EBOV challenge, with a survival rate of 90%–100%. In contrast, the $CD45^{100\%}$, $CD45^{0\%}$, $CSV10^{+/-}$, and $CSV10^{+/+}$ mice did not survive EBOV challenge (Figure 1B). However, a delay in the mean time to death was observed in $CD45^{0\%}$ and CSV10 (+/− and +/+) mice.

Functional Consequences of Reduced CD45 Expression

To investigate whether reduced CD45 expression affects the entry, replication, or budding of the virus, splenocytes harvested from $CD45^{100\%}$, $CD45^{62\%}$ and $CD45P^{0\%}$ mice were infected ex vivo with EBOV, and viral titers were measured by plaque assay. As shown in Figure 1C, similar viral titers were obtained from splenocytes expressing different levels of CD45. Thus, changes in CD45 expression levels had no effect on viral replication.

The control and clearance of EBOV infection has been shown to correlate with effective humoral and T-cell-mediated responses, as mice vaccinated with Ebola virus-like particles (VLPs) require both B cells and CD^{*+} T cells for protection against mouse-adapted EBOV infection (Warfield et al., 2005). Accordingly, mice that survived EBOV challenge developed EBOV-specific antibodies (Figure 1D), and upon rechallenge with EBOV, a 100% survival rate (20/20) was observed for mice expressing a range of reduced CD45 levels (data not shown). Furthermore, $CD8^+$ T cell responses against defined EBOV, GP, NP, and VP40 epitopes were observed by day 7 post-EBOV infection (data not shown).

Protective Immunity in EBOV-Infected $CD45^{62\%}$ Mice

To understand the role of reduced CD45 expression during EBOV infection, we performed a time course study to monitor functional and cellular changes at both the transcript and protein levels (Figure 2A). Chemo/cytokine analysis of blood plasma indicated that MCP-1, FGF, IFN-γ, IL-4, IL-10, and IL-12 were induced upon viral infection (day 3 and/or 5) in both the $CD45^{62\%}$ and $CD45^{100\%}$ mice (Figure 2B). A significant decrease ($p < 0.05$) in IL-4 levels was observed 3 days after infection in $CD45^{62\%}$ mice versus $CD45^{100\%}$ mice, and the levels of this cytokine were abolished by day 5 in both groups of mice. The levels of the regulatory cytokine IL-10 at day 3 were higher in $CD45^{100\%}$ compared to $CD45^{62\%}$ and completely abrogated by day 5 postinfection in $CD45^{100\%}$ mice. Thus, these data suggested that the initiation of optimal immunity in $CD45^{62\%}$ mice was achieved by regulated expression of IL-10 upon EBOV infection, which otherwise can suppress ongoing antiviral immunity (Couper et al., 2008).

Moreover, staining of splenocytes showed a significant increase ($p < 0.05$) in the percentage of $CD11b^+$ $CD11c^-$ macrophages and $Ly6G^+$ granulocytes at 5 days after EBOV challenge in $CD45^{62\%}$ versus $CD45^{100\%}$ mice (Figure 2C). In blood, the percentage of activated $CD8^+$ $CD44^{high+}$ T cells increased dramatically ($p < 0.05$) at 5 days after challenge in $CD45^{62\%}$ mice when compared to $CD45^{100\%}$ mice (Figure 2D). The $CD45^{62\%}$ mice had constitutively elevated percentages of activated T cells, and these increased levels were maintained through day 5 in both spleen and blood. The time course study suggested that the immune responses in $CD45^{62\%}$ mice were altered following EBOV infection, resulting in an increased percentage of macrophages and granulocytes. Collectively, these data suggested that reduced CD45 levels might heighten the homeostasis of immune cells in favor of protective immunity during filoviral infection.

Viral Clearance and Reduced Apoptosis in EBOV-Infected $CD45^{62\%}$ Mice

EBOV clearance is controlled by functional innate and adaptive immune responses (Mohamadzadeh et al., 2007). Accordingly,

Please cite this article in press as: Panchal et al., Reduced Levels of Protein Tyrosine Phosphatase CD45 Protect Mice from the Lethal Effects of Ebola Virus Infection, Cell Host & Microbe (2009), doi:10.1016/j.chom.2009.07.003

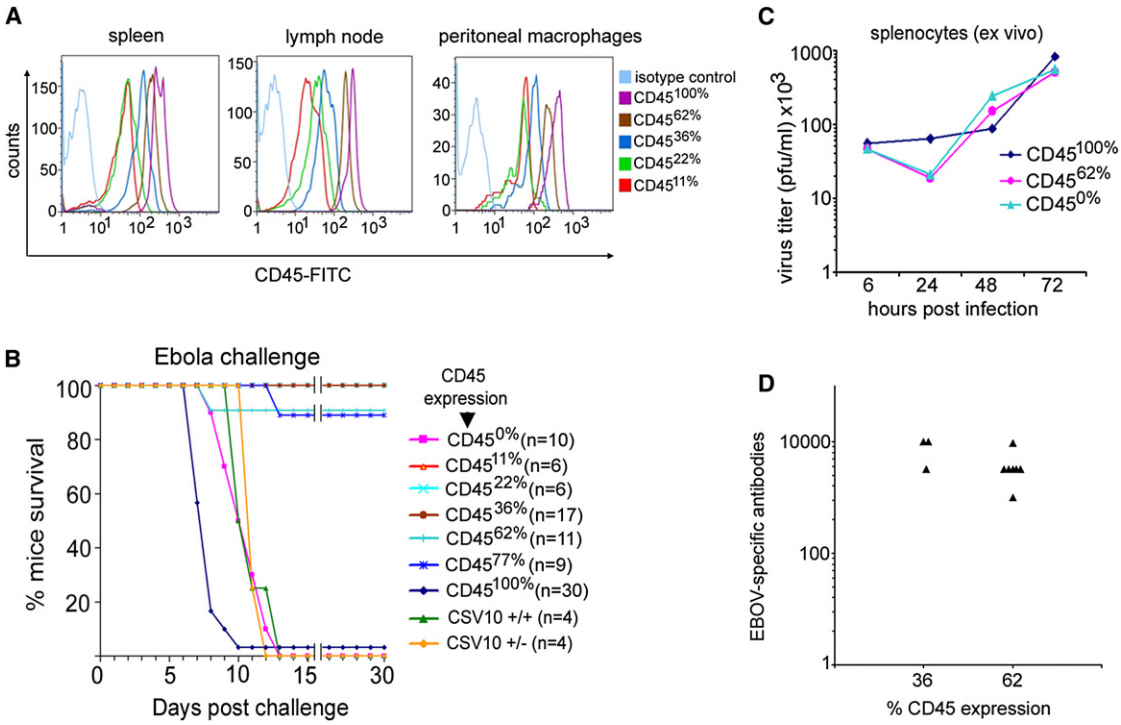

Figure 1. Reduced CD45 Expression Protects EBOV-Infected Mice but Does Not Affect Viral Replication Ex Vivo

(A) CD45 expression levels of transgenic and heterozygous mice. Peritoneal macrophages and cells isolated from spleen or lymph node from the wild-type ($CD45^{100\%}$) and mice with reduced CD45 expression levels were stained with FITC-conjugated anti-CD45 antibody and were analyzed by flow cytometry.

(B) Mice expressing reduced levels of CD45 (11%–77% CD45 expression) were protected following infection with EBOV. The $CD45^{100\%}$, $CD45^{0\%}$, or CSV10 (+/+, 100%) or CSV10 (+/−, 62%) mice having inactivated CD45 phosphatase activity did not survive EBOV infection.

(C) Splenocytes harvested from 100%, 62%, and 0% CD45-expressing mice were infected (MOI = 1) ex vivo with mouse-adapted EBOV. At times 6, 24, 48, and 72 hr, supernatant was harvested and viral titers were determined by traditional plaque assays (Moe et al., 1981).

(D) Mice with reduced CD45 expression that survived EBOV challenge generated serum-EBOV-specific antibody responses.

a time course study showed that, at 7 days following EBOV challenge, the $CD45^{62\%}$ mice had reduced viral titers in the kidney, liver, spleen, and serum (Figure 3A). By day 10, no EBOV was detected in the different tissues of the $CD45^{62\%}$ mice, suggesting that a robust immune response was elicited in these mice (Figure 3A). Similarly, immunohistochemical staining of liver, spleen, and lymph nodes showed reduced EBOV antigen and increased cellularity of lymphocytes in the $CD45^{62\%}$ mice at 7 days following EBOV challenge (Figure 3B). No EBOV antigen was detected at 10 days (Figure 3C) or 30 days (Figure 3D) following EBOV challenge. Viral clearance was likewise observed in all other reduced-CD45-expressing mice that survived EBOV challenge (data not shown). In contrast, the $CD45^{100\%}$ mice failed to clear the virus and succumbed to the pathogen between 7 and 8 days following EBOV challenge. These studies indicated that the cellular integrity and observed active cellular homeostasis might have resulted in the viral clearance in $CD45^{62\%}$ mice.

EBOV infection is also associated with induced apoptosis of lymphocytes (Mohamadzadeh et al., 2007). To detect apoptosis, we stained tissues from the time course study using the TUNEL technique. TUNEL staining of spleen samples from $CD45^{100\%}$ and $CD45^{62\%}$ mice on day 5 (Figure 3E) following EBOV challenge revealed apoptotic cells in red pulp areas where extramedullary hematopoiesis (EMH) normally occurs. In the EMH regions, significant cell depletion was observed on day 5 following infection in both groups of mice, suggesting prior loss or migration of cells. In the liver at day 5, there was no significant apoptosis observed in either group of mice (Figure 3F). However, by day 7, markedly increased (38-fold change compared to day 5) apoptosis was seen in the liver of $CD45^{100\%}$ mice. In contrast, there was much less apoptosis in the $CD45^{62\%}$ at day 7 in both the liver and spleen. These findings were confirmed by analyzing apoptosis characterized by the presence of pyknotic nuclei using H&E staining (data not shown) and by quantitation of the TUNEL-positive cells from the immunohistochemical images (Figure 3G). These data suggested that reduced CD45 expression levels may regulate EBOV-induced apoptosis of these cells.

Critical Role of $CD8^+$ T Cells in Protecting $CD45^{62\%}$ Mice against EBOV Challenge

Two independent approaches were taken to identify the critical cellular players responsible for the protective response in the $CD45^{62\%}$ mice. In one approach, Rag knockout mice expressing 62% or 100% CD45 levels were challenged with EBOV. Neither group of mice survived EBOV challenge, suggesting that B and/or T cells are required for the mice to survive EBOV infection (Figure 4A). In the second approach, lymphocyte subsets were depleted in vivo using cell-type-specific antibodies prior to EBOV infection. As shown in Figure 4B, depletion of all T cells

Please cite this article in press as: Panchal et al., Reduced Levels of Protein Tyrosine Phosphatase CD45 Protect Mice from the Lethal Effects of Ebola Virus Infection, Cell Host & Microbe (2009), doi:10.1016/j.chom.2009.07.003

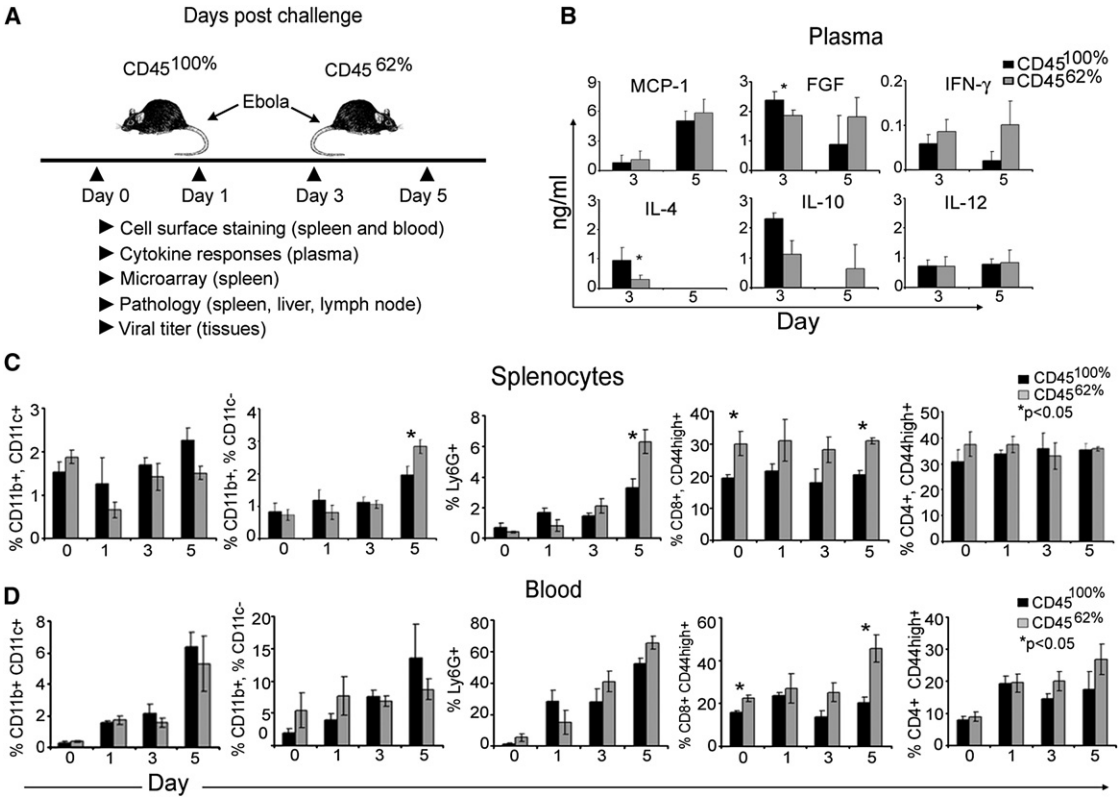

Figure 2. Timeline of Cell-Profiling Studies

(A) Schematic diagram of a timeline study wherein CD45$^{100\%}$ and CD45$^{62\%}$ mice were either not infected or infected with 1000 pfu of mouse-adapted EBOV. At days 0, 1, 3, and 5, four mice per group were euthanized, various tissues were harvested, and blood was collected.

(B) Cytokine and chemokine levels from the plasma of CD45$^{100\%}$ and CD45$^{62\%}$ mice euthanized at days 0, 1, 3, and 5 post-EBOV infection were measured using the cytokine 20-plex luminex kit. Only those samples that showed any detectable levels of cytokines were included. The data represent the averages of four mice per group per time point ± SD.

(C) Splenocytes isolated from mice euthanized at days 0, 1, 3, and 5 following EBOV infection were stained for cell-surface and activation markers and were analyzed by flow cytometry. The data represent the averages of four mice per group per time point ± SE.

(D) Blood cells collected from mice euthanized at days 0, 1, 3, and 5 post-EBOV infection were stained for cell-surface and activation markers and were analyzed by flow cytometry. The data represent the averages of four mice per group per time point ± SE.

using CD90.2 (a Thy1.2 antibody) or depletion of CD8+ T cells resulted in increased mortality of the CD45$^{62\%}$ mice to EBOV challenge. In contrast, minimal susceptibility was observed following CD4+ T cell depletion, whereas depletion of NK subsets with NK1.1 antibody or treatment with IgG_2b control antibody had no effect on mice survival.

Activated CD8$^+$ T cells secrete interferon γ (IFN-γ) to modulate immune function. To determine whether IFN-γ played a role in protection of CD45$^{62\%}$ mice from EBOV infection, a neutralizing IFN-γ antibody was used. Depletion of IFN-γ resulted in susceptibility of CD45$^{62\%}$ mice to EBOV infection (Figure 4C), suggesting that this cytokine played a critical role in induced T cell immune responses against EBOV in CD45$^{62\%}$ mice. Together, these studies suggested that CD8$^+$ T cells and IFN-γ play a pivotal role in controlling infection in the CD45$^{62\%}$ mice.

Early Control of Gene Regulation in EBOV-Infected CD45$^{62\%}$ Mice

To gain insight into the changes in gene regulation elicited upon EBOV infection, we used Affymetrix gene chip arrays to compare gene expression in splenocytes from CD45$^{100\%}$ and CD45$^{62\%}$ mice. Based on gene expression patterns, the variable genes were grouped into 16 clusters (Figure 5A). The clusters contained genes associated with cellular immune processes, signaling, cell-cycle, complement coagulation cascade, biosynthesis/metabolism, ubiquitous genes involved in several cascades, and genes of unknown function (Table S1 available online). Interestingly, gene expression at day 1 following EBOV challenge in CD45$^{100\%}$ mice was more similar to day 3 postinfection than preinfection. In contrast, at day 1 following EBOV infection, the CD45$^{62\%}$ mice maintained gene expression patterns similar to day 0. The differences in gene expression patterns between the CD45$^{100\%}$ and CD45$^{62\%}$ splenocytes were less apparent at day 3 following infection, and by days 5 and 7, they became very similar. At day 9, when wild-type mice had succumbed to the disease, the pattern in CD45$^{62\%}$ mice remained similar to the day 7 patterns of CD45$^{100\%}$ and CD45$^{62\%}$ mice. The pattern at days 11 and 13 in the CD45$^{62\%}$ mice became similar to that of day 0 CD45$^{100\%}$ or CD45$^{62\%}$ mice. These results suggested that, in CD45$^{100\%}$ mice, subversion of the cell transcriptional machinery during the early stages of EBOV infection (day 1) might represent a major factor leading to death of the mice. In

Please cite this article in press as: Panchal et al., Reduced Levels of Protein Tyrosine Phosphatase CD45 Protect Mice from the Lethal Effects of Ebola Virus Infection, Cell Host & Microbe (2009), doi:10.1016/j.chom.2009.07.003

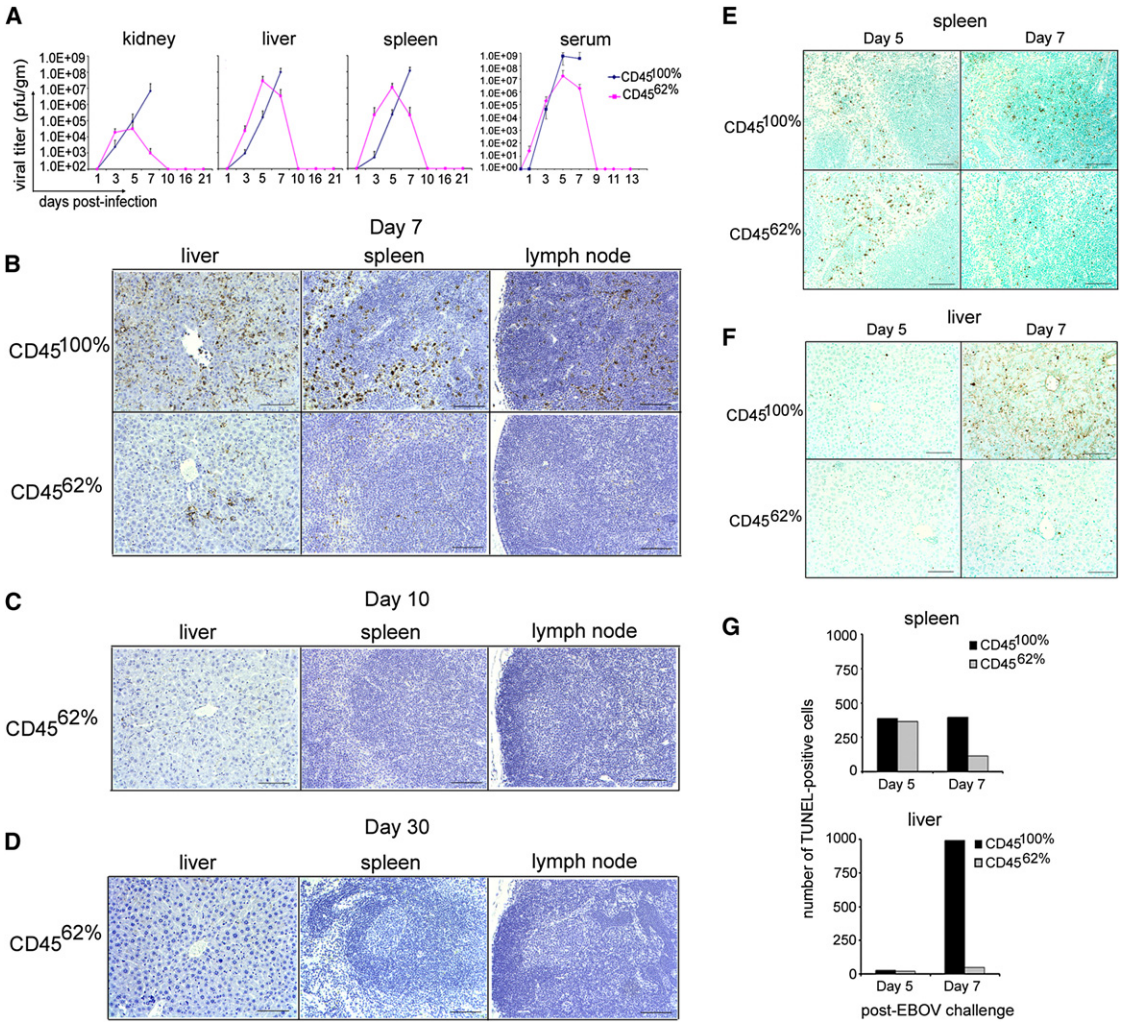

Figure 3. Viral Clearance and Reduced Apoptosis in EBOV-Infected CD45$^{62\%}$ Mice

(A) Single cells were derived from kidney, liver, spleen, and serum of the EBOV-infected CD45$^{100\%}$ and CD45$^{62\%}$ mice on days 1, 3, 5, 7, 10, 16, and 21. Viral titers were measured using plaque assays (Moe et al., 1981). The data represent averages of four mice per group per time point ± SD.

(B) Immunohistochemical images of liver, spleen, and mesenteric lymph node from CD45$^{100\%}$ and CD45$^{62\%}$ mice euthanized at 7 days after EBOV infection and stained with anti-EBOV antibody. Scale bar, 100 um; 20× magnification.

(C) CD45$^{62\%}$ mice euthanized at 10 days after EBOV infection and stained with anti-EBOV antibody. Scale bar, 100 um; 20× magnification.

(D) CD45$^{62\%}$ mice euthanized at 30 days after EBOV infection and stained with anti-EBOV antibody. Scale bar, 100 um; 20× magnification.

(E) TUNEL staining of spleen from CD45$^{100\%}$ and CD45$^{62\%}$ mice euthanized at 5 and 7 days after EBOV challenge. Scale bar, 100 μm; 20× magnification.

(F) TUNEL staining of liver from CD45$^{100\%}$ and CD45$^{62\%}$ mice euthanized at 5 and 7 days after EBOV challenge. Scale bar, 100 μm; 20× magnification.

(G) For quantitation of TUNEL staining, we acquired histology images as three separate black and white photos taken successively with a blue, green, and red filter on a Nikon E800 microscope with a SPOT RT camera. The color overlay function of MetaMorph imaging software (Molecular Devices Corporation, Downingtown, PA) was used to recombine the separate black and white images into a color image. To quantitate the number of apoptotic cells, black and white images taken with a green filter were each adjusted to an identical threshold value. The MetaMorph software "count cells" application was used to enumerate TUNEL-positive cells.

CD45$^{62\%}$ mice, early control of gene regulation likely provided the appropriate antiviral responses leading to regulated inflammation, immune costimulation, and survival.

Functional and Canonical Pathways Modulated by EBOV-Infected CD45$^{62\%}$ Mice

To gain further insight into the changes in gene regulation upon EBOV infection, we examined Gene Ontology (GO) Biological Process annotations for genes that were significantly different between CD45$^{100\%}$ and CD45$^{62\%}$ mice at each time point (posterior probability of no change, $p < 1E-10$ using the empirical Bayes; Kendziorski et al., 2003). The primary biological functions that were significantly enriched ($p < 0.05$ by Fisher's exact test) among genes differentially expressed between the CD45$^{100\%}$ and CD45$^{62\%}$ ($p < 1E-10$) over the course of EBOV infection included immune and inflammatory responses, chemotaxis, cell cycle, apoptosis, and antiapoptosis (Table 2). In particular, the number of differentially expressed genes

Please cite this article in press as: Panchal et al., Reduced Levels of Protein Tyrosine Phosphatase CD45 Protect Mice from the Lethal Effects of Ebola Virus Infection, Cell Host & Microbe (2009), doi:10.1016/j.chom.2009.07.003

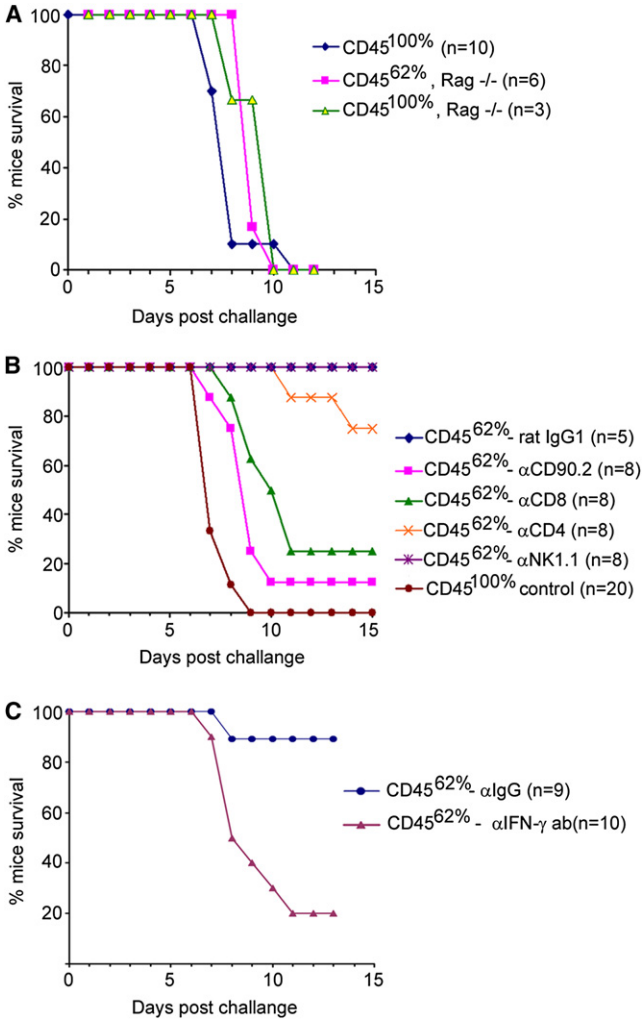

Figure 4. CD45$^{62\%}$ Mice Depleted of T Cells or IFN-γ Succumbed to EBOV Infection

(A) Wild-type control mice and Rag$^{-/-}$ mice expressing either 100% or 65% CD45 levels all succumbed to EBOV challenge.

(B) CD45$^{62\%}$ mice depleted of CD8^{+} T cells or all T cells (CD90.2) using specific antibodies succumbed to EBOV infection.

(C) CD45$^{62\%}$ mice treated with IFN-γ-neutralizing antibody succumbed to EBOV infection.

associated with immune and inflammatory responses and chemotaxis were high on day 0 (before challenge) and day 5 following EBOV infection. Cell-cycle genes were significantly ($p = 3.0E - 04$) enriched at day 1, whereas an increased number of apoptotic and antiapoptotic genes were observed late in the infection process (day 7). This gene expression data supported our tissue pathology observations that indicated increased homeostasis and cellularity, as well as a concomitant increase in apoptosis on day 5 and a decreased apoptosis on day 7 in the CD45$^{62\%}$ mice during the middle to late stages of EBOV infection.

Additionally, the expression results were analyzed using the Ingenuity Pathway Analysis software (Ingenuity Systems, http://www.ingenuity.com). Ingenuity-defined canonical signaling pathways that were overrepresented (Fisher's exact test) among genes that differed between the CD45$^{62\%}$ and CD45$^{100\%}$ mice at day 1 after infection included IL-10 signaling, LXR/RXR activation, p53 signaling, and cell-cycle regulation pathways (Figure 5B). Of great interest was the IL-10 signaling pathway, as increased levels of this cytokine have previously been reported in EBOV-infected humans during the first few days of clinical illness. However, they all succumbed to the lethal infection (Hutchinson and Rollin, 2007; Villinger et al., 1999). Our array data showed reduced *IL-10* expression throughout the course of EBOV infection in the CD45$^{62\%}$ mice when compared to CD45$^{100\%}$ mice (Figure 5C). A statistically significant reduction in *IL-10* expression was observed only at days 3 ($p = 7.8E - 5$ by empirical Bayes; Kendziorski et al., 2003) and 7 ($p = 0.029$) following EBOV infection. However, a significant fraction of the genes within the IL-10-signaling pathway exhibited altered expression levels in the CD45$^{62\%}$ mice at day 1 ($p = 6.0E - 4$ by Fisher's exact test; Figure 6A). Gene array analysis thus suggests that reduced CD45 levels may, in part, regulate immune mechanisms via IL-10 signaling, which is important for regulating or suppressing T cell responses.

DISCUSSION

In this study, we show that a range of reduced CD45 expression levels (11%–77%) resulted in a protective effect that allowed mice to survive EBOV infection. Furthermore, this effect was shown to be dependent on CD45 phosphatase activity, as mice with reduced expression levels of phosphatase-inactive CD45 succumb to the pathogen. CD45$^{62\%}$ mice demonstrated reduced viral titers in the kidney, liver, spleen, and serum 7 days following EBOV challenge, with no EBOV detected by day 10, suggesting that an unusually robust immune response elicited in CD45$^{62\%}$ mice might have allowed them to control the viral infection and subsequently survive EBOV challenge. Furthermore, significantly less cellular apoptosis was observed in both the livers and spleens of these mice relative to CD45$^{100\%}$ mice.

Based on prior studies, it is clear that quick onset of innate immune responses matched with balanced inflammation (Mohamadzadeh et al., 2006) and T cell immunity (particularly CD8^{+} T cells) are pivotal for the clearance of EBOV infection (Bradfute et al., 2008). Our data indicated that CD8^{+} T cells and IFN-γ are critical players in clearing EBOV infection in CD45$^{62\%}$ mice. We observed that CD45$^{62\%}$ mice had constitutively elevated percentages of activated T cells and macrophages and that these increased levels were maintained through day 5 in both the spleen and blood. In addition, our analysis suggested that intermediate CD45 levels might have controlled the inflammatory mechanisms by way of lowered IL-10 expression, which would lead to a heightened T cell response. Furthermore, depletion of all T cells, CD8^{+} T cells, or IFN-γ (a product of CD8^{+} T cells) increased mortality of CD45$^{62\%}$ mice following EBOV challenge. It is known that a CD8^{+} T cell immune response is generated even during lethal EBOV infections, and adoptive transfer of these cells protects naive mice from EBOV challenge (Bradfute et al., 2008). Our studies are consistent with a model in which the function and development of EBOV-specific CD8^{+} T cells is accelerated in the CD45$^{62\%}$ mice.

Please cite this article in press as: Panchal et al., Reduced Levels of Protein Tyrosine Phosphatase CD45 Protect Mice from the Lethal Effects of Ebola Virus Infection, Cell Host & Microbe (2009), doi:10.1016/j.chom.2009.07.003

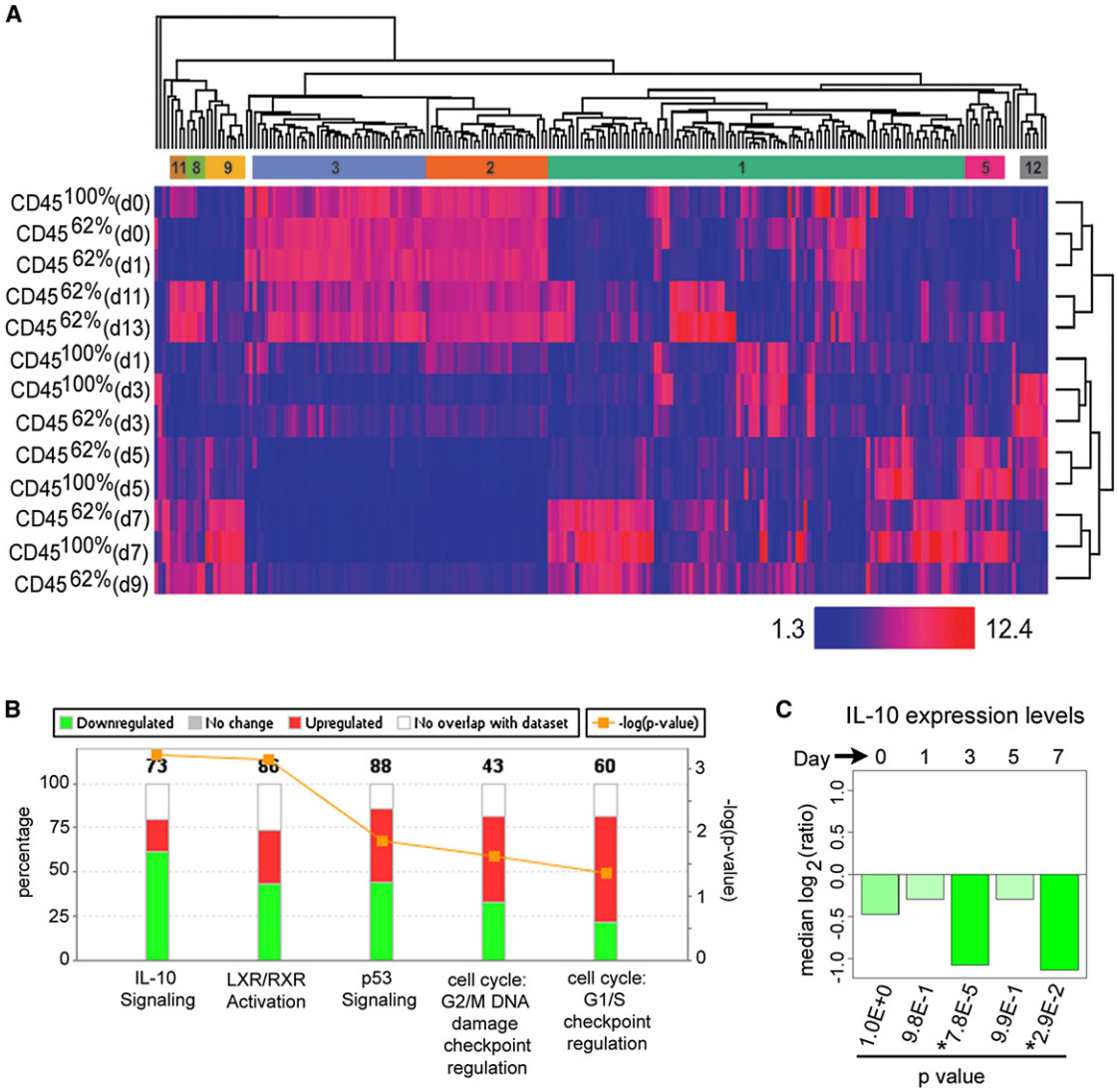

Figure 5. Early Control of Gene Expression in EBOV-Infected CD45$^{62\%}$ Mice

(A) Heat map showing variable genes in splenocytes of CD45$^{100\%}$ and/or CD45$^{62\%}$ mice at days 0, 1, 3, 5, 7, 9, 11, and 13 (d0, d1, d3, d5, d7, d9, d11, and d13) post-EBOV infection. The heat map is of $\log B_{2B}$ expression values in splenocytes for 227 genes with coefficient of variation > 1.4. Genes and samples are arranged by dendrograms created with agglomerative nesting, and genes are assigned to 16 main clusters (colored bars). Clusters smaller than three genes are not numbered (white bars).

(B) The five main canonical pathways that were most significantly enriched among the genes with different expression levels in CD45$^{100\%}$ and CD45$^{62\%}$ mice at 1 day after infection and identified from the Ingenuity Pathway Analysis library.

(C) Expression differences between CD45$^{100\%}$ and CD45$^{62\%}$ for IL-10 during EBOV infection. Values are expressed as $\log_2$(CD45$^{62\%}$/CD45$^{100\%}$). P values represent posterior probability of no change by empirical Bayes. The statistically significant p values are shown with an asterisk (*).

Exactly how CD45$^{62\%}$ mice generate this unusually rapid/robust immune response is uncertain. However, our microarray analysis suggests that CD45$^{62\%}$ mice were able to bypass the dramatic downregulation of gene expression elicited in CD45$^{100\%}$ mice following EBOV challenge. Specifically, gene expression in clusters 2 and 3 was observed to be downregulated on day 1 following EBOV challenge in CD45$^{100\%}$ mice. In contrast, on day 1 following EBOV infection, CD45$^{62\%}$ mice maintained gene expression patterns similar to those observed on day 0. These results indicated that lower expression levels of CD45 prevented EBOV subversion of the cell transcriptional machinery during the early stages of infection, suggesting that failure to control transcriptional regulation may represent a major factor leading to death in CD45$^{100\%}$ mice. These findings could be the basis for future studies to determine whether CD45 may play a controlling role in the wide variety of outcomes of Ebola virus infection, such as the resistance of mice to natural filovirus isolates.

In addition to the observed increased number of CD8$^+$ T cells in CD45$^{62\%}$ mice, our gene expression analysis indicated that increased *trans*-endothelial migration of effector CD8$^+$ T cells to sites of viral infection might be influenced by CD45 levels.

Please cite this article in press as: Panchal et al., Reduced Levels of Protein Tyrosine Phosphatase CD45 Protect Mice from the Lethal Effects of Ebola Virus Infection, Cell Host & Microbe (2009), doi:10.1016/j.chom.2009.07.003

Table 2. Selected GO Biological Process Annotations

	Day 0		Day 1		Day 3		Day 5		Day 7	
GO Term	P	Genes	P	Genes	P	Genes	P	Genes	P	Genes
Immune response	4.3E − 06[a]	10	1.9E − 01	6	3.0E − 01	6	5.1E − 04[a]	9	5.4E − 01	1
Inflammatory response	1.2E − 12[a]	13	1.4E − 01	4	6.8E − 01	2	1.9E − 04[a]	7	1.0E − 00	0
Chemotaxis	6.5E − 05[a]	5	8.1E − 02[a]	3	6.9E − 01	1	3.5E − 04[a]	5	1.0E − 00	0
Antiapoptosis	2.8E − 01	1	5.4E − 0 1	1	6.0E − 01	1	7.9E − 02	2	4.4E − 04[a]	3
Apoptosis	2.7E − 01	4	6.0E − 01	6	1.9E − 01	10	5.3E − 01	4	3.1E − 02[a]	4
Cell cycle	3.1E − 01	4	3.0E − 04[a]	17	1.5E − 01	11	5.7E − 01	4	1.4E − 01	3

Enrichment of selected GO Biological Process annotations among genes differentially expressed between $CD45^{100\%}$ and $CD45^{62\%}$ mice ($p < 1E - 10$). The number of genes, with indicated GO annotations, and one-tailed Fisher's exact p value for overrepresentation within the set of differentially expressed genes are shown for each time point.

[a] $p < 0.05$.

T cell migration is regulated by differential expression of various adhesion molecules and chemokines (Thomsen et al., 2003). In our study, EBOV infection did not modulate the gene expression of integrin family members or selectins in either the $CD45^{100\%}$ or $CD45^{62\%}$ mice (data not shown). However, expression of intracellular adhesion molecule 4 (*ICAM4*) was significantly higher in $CD45^{62\%}$ compared to $CD45^{100\%}$ at days 1 ($p = 3.7E - 08$), 3 ($p = 1.0E - 23$), and 5 ($p = 1.3E - 07$) following EBOV challenge, which may have reduced or delayed T cell activation and differentiation (Figure 6B). In contrast, the vascular cell adhesion molecule-1 (*VCAM-1*) expression was lower in $CD45^{62\%}$ at days 1 and 5 following EBOV infection than in $CD45^{100\%}$ mice. Furthermore, $CD45^{62\%}$ mice had significantly reduced expression of chemokine receptors, including *CCR1* (days 0 and 1), *CCR3* (days 0, 1, and 3), *CXCL1* (days 0 and 1), and *CXCL3* (days 0, 1, 5, and 7), following EBOV challenge (Figure 6B). In contrast, expression of *CXCR3* was significantly higher ($p = 7.5E - 04$) at day 0 in $CD45^{62\%}$ mice but declined to that of $CD45^{100\%}$ mice on days 1, 3, 5, and 7 following EBOV infection. Thus, a balance between the expression levels of the appropriate adhesion molecules and chemokines may critically regulate lymphocyte migration to the site of infection and thereby influence the efficiency of the antiviral response in $CD45^{62\%}$ mice.

How CD45 expression levels influence the antiviral response and its underlying molecular mechanism is unclear. Depending on the stimulus and the cell type, the role of CD45 in signal transduction varies. For example, the role of CD45 in regulating activation of Src family kinases, such as $p56/59^{hck}$ and $p53/56^{lyn}$ in macrophages, is distinct from its role in regulating the leukocyte-specific protein tyrosine kinase $p56^{lck}$ during lymphocyte antigen receptor signaling. Recently, McNeill et al. (McNeill et al., 2007) showed that differential CD45 expression levels appear to control the sensitivity of T cell signaling. Wild-type expression levels of a single CD45RO isoform were critical for dephosphorylation of pTyr394 of $p56^{lck}$, whereas intermediate levels of the CD45RO isoform were effective at dephosphorylating the pTyr-505 of $p56^{lck}$. In our study, the observed protective immunity elicited by intermediate CD45 levels may be a consequence of differential regulation of phosphorylation (at pTyr-505 and pTyr-394) of $p56^{lck}$ (McNeill et al., 2007; Zamoyska, 2007). In vitro and in vivo mechanistic studies that monitor changes in the sensitivity of Src signaling in different cell types before and after EBOV infection, although technically challenging, would be the key to understanding how differential CD45 levels regulate innate and adaptive immune responses.

The activities of virus-induced cellular mediators, including IFNs, cytokines, and intracellular signaling molecules, are controlled at multiple levels to provide an effective antiviral state. Based on our results, we propose a model wherein reduced CD45 expression regulates multiple mechanisms at different stages of EBOV infection (Figure 6C). Our studies suggest that homeostatic immune cell proliferation, enhanced cell trafficking and migration, regulated inflammation, and early control of gene expression related to disease pathogenesis collectively may contribute to reduced apoptosis, viral clearance, and survival of the EBOV-infected $CD45^{62\%}$ mice. Furthermore, the timing, location, interaction with binding partners, and signal intensity of the cellular, molecular, and immune responses all act in concert with the development of the host protective regulatory response in the $CD45^{62\%}$ mice challenged with EBOV.

Previously, we showed that intermediate levels of CD45 expression reduced apoptosis of *B. anthracis*-infected macrophages and protected mice from anthrax pathogenesis (Panchal et al., 2009). Mechanism-based studies suggested that the protection provided by reduced CD45 levels resulted from regulated immune cell homeostasis that might have diminished the impact of apoptosis during the infection. Thus, in both the Ebola and *B. anthracis* infection models, reduced CD45 expression seems to regulate apoptosis by way of immune function. Although it is presumed that diverse pathogens elicit divergent molecular and cellular responses in mammalian hosts, these studies suggest that these phylogenetically distant pathogens likely converge at a singular, CD45-mediated process. However, whether or not similar gene regulatory events and/or signaling pathways are influenced by reduced CD45 expression in these distinct infection models remains to be investigated.

The similar ability of reduced CD45 levels to confer resistance to these two dissimilar pathogens may prove to be of extraordinary importance, as it highlights CD45 as a primary target for rational drug design. The therapeutic benefits of totally eliminating CD45 protein expression have been shown in Coxsackie B3 viral infections that cause severe immunopathologies (Irie-Sasaki et al., 2001), whereas anti-CD45RO antibodies suppress the replication of human immunodeficiency virus in cultured human microglial cells (Kim et al., 2006). On the contrary, our

Please cite this article in press as: Panchal et al., Reduced Levels of Protein Tyrosine Phosphatase CD45 Protect Mice from the Lethal Effects of Ebola Virus Infection, Cell Host & Microbe (2009), doi:10.1016/j.chom.2009.07.003

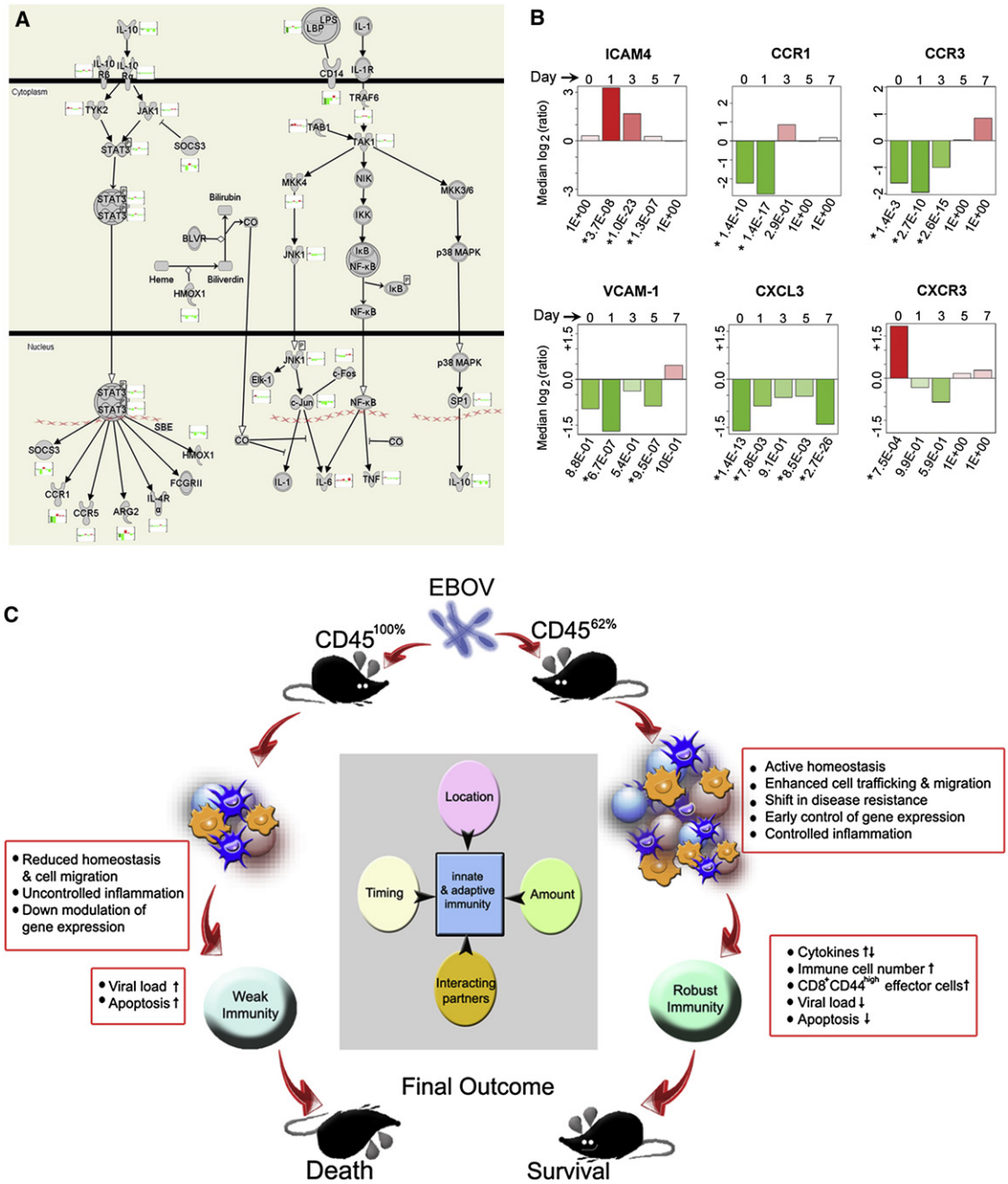

Figure 6. Proposed Model of How Reduced Expression of CD45 Elicits a Protective Response following EBOV Challenge

(A) IL-10-signaling pathway. Bar charts adjacent to the molecules display the $\log_2$ ratio of $CD45^{62\%}$ to $CD45^{100\%}$ expression levels over time.

(B) Expression differences between $CD45^{100\%}$ and $CD45^{62\%}$ for ICAM4, CCR1, CCR3, VCAM-1, CXCL3, and CXCR3 during EBOV infection. Values are expressed as $\log_2(CD45^{62\%}/CD45^{100\%})$. P values represent posterior probability of no change by empirical Bayes. The statistically significant p values are shown with an asterisk (*).

(C) Effective immunity, homeostatic immune cell proliferation, and enhanced cell migration observed in $CD45^{62\%}$ mice collectively contribute to reduced apoptosis, viral clearance, and subsequent survival of mice challenged with EBOV. The timing, location, interaction with binding partners, and signal intensity of the cellular, molecular, and immune responses is critical for the protective immunity in the reduced CD45-expressing mice.

studies show that reduced expression, but not complete knockout, of CD45 is critical for the protective phenotype following either EBOV or *B. anthracis* infection. The availability of a mouse model expressing differential levels of CD45 (Virts et al., 2003; Wallace et al., 1997) would allow us to further explore the effects and role of altered CD45 levels in these infectious disease models. Furthermore, therapeutic targeting of the downstream effector molecules of CD45 in combination with CD45

itself may prove beneficial for the development of host-based therapeutics. Importantly, the functional studies described here provide evidence that this enzyme is a promising target for host-based therapeutics for the treatment of a broad range of infectious diseases.

EXPERIMENTAL PROCEDURES

Transgenic and Heterozygous Mice

All mice in this study are of the C57BL/6 genetic background. The heterozygous $CD45^{62\%}$ mice have one exon-9 knockout allele and one wild-type allele. The CD45 transgenic mice were produced using a *CD45* minigene construct containing cDNA from exons 1b-3, the genomic sequence from exon 3 to 9 (which includes the variably spliced exons and surrounding introns), and cDNA from exon 9 through the polyadenylation signal region in exon 33, as described previously (Virts et al., 2003; Virts and Raschke, 2001). Three founder transgenic mice were obtained (B, F, and H), and each was bred to the exon-9 disrupted CD45 knockout strain (Byth et al., 1996) (obtained from Jackson Labs, Bar Harbor, ME). The properties of the F strain have been reported by Virts et al. (Virts et al., 2003) and include the same regulated, cell-type-specific CD45 isoform expression as observed in wild-type mice. Transgenic mice containing a point mutation (C817S) in the membrane-proximal phosphatase domain of the *CD45* minigene were also produced. This mutation has been shown to abolish CD45 PTPase activity in vitro (Desai et al., 1994), and this has been confirmed in ex vivo studies (W.C.R. et al., unpublished data). The CSV10 transgenic mice were generated using the C817S mutant minigene, and the transgene locus was bred onto the CD45 knockout background. A more complete description of the properties of all transgenic strains in the knockout background, including those that express an inactive CD45 protein, will be published elsewhere (W.C.R. et al., unpublished data). The cell-surface expression levels of CD45 in all of the knockdown mice were determined using flow cytometry by comparison of the mean fluorescence intensities of the lymphocyte populations to those of $CD45^{100\%}$ wild-type and $CD45^{0\%}$ knockout mice (Virts et al., 2003). The expression level of CSV10 transgenic mice containing one copy of the transgene insertion locus ($CSV10^{+/-}$) was 62%–65%, a level similar to that expressed by $CD45^{62\%}$ heterozygous mice.

The Rag knockout ($Rag^{-/-}$) mice were obtained from Dr. Linda Bradley (Sidney Kimmel Cancer Center, San Diego, CA). To generate $CD45^{62\%}$ mice in the Rag knockout background, $CD45^{62\%}$ heterozygous mice ($CD45^{62\%}$, $Rag^{+/+}$) were mated with Rag knockout mice ($CD45^{100\%}$, $Rag^{-/-}$), and offspring with 62% expression of CD45 were mated with $Rag^{-/-}$ mice. The resulting litters were screened by flow cytometric analysis of blood samples for 62% CD45 expression and the $Rag^{-/-}$ phenotype (very low numbers of $CD19^{+}$ cells).

Animal Studies

Mice (8- to 10-week-old) were used in this study and included both males and females. For in vivo Ebola studies, mice were challenged via intraperitoneal (i.p.) route with 1000 pfu of mouse-adapted Ebola Zaire virus. Mice that survived EBOV challenge were either rechallenged or they had their blood collected to measure anti-EBOV antibody levels in the serum by ELISA, and their tissues were harvested for pathology, T cell responses, and viral titer measurements (Warfield et al., 2006).

All research was conducted under an approved protocol and in compliance with the Animal Welfare Act, as well as other federal statutes and regulations related to animals and experiments involving animals, and adhered to principles stated in the *Guide for the Care and Use of Laboratory Animals*, National Research Council 1996. The facility where this research was conducted is fully accredited by the Association for Assessment and Accreditation of Laboratory Animal Care International.

Flow Cytometry

Antibodies used for FACS analysis were purchased from BD PharMingen (San Diego, CA) unless otherwise noted. Antibodies used were directly conjugated to FITC, PE, APC, PerCP, or PECy5. Clones used in these studies included CD45 (30-F11), CD3 (17A2), CD4 (RM4-5), CD8 (53-6.7), CD11b (M1/70), CD11c (N418, eBioscience), CD19 (1D3), NK1.1 (PK136, eBioscience), MHC I (28-14-8), MHC II (M5/114.15.2), CD44 (IM7), and Ly6G (1A8). Cells (1×10^6) were resuspended in Fc block (anti CD16/CD32 antibody diluted in RPMI medium containing 10% FBS), incubated on ice for 30 min, centrifuged, and stained with appropriate combinations of labeled antibodies. After incubation on ice for 60 min, cells were washed and resuspended in 10% formaldehyde. FACS analysis was performed using a FACSCalibur flow cytometer (BD Biosciences). Data were analyzed using FlowJo software. Statistical analyses of the data were performed using the two-tailed Student's t test.

Cytokine Detection

Plasma separated from heparinized blood was analyzed for secreted cytokines using the mouse cytokine 20-plex AB Bead kit (Biosource). All analyses were performed on a Bio-Plex workstation using accompanying software (Bio-Rad). Statistical analysis of the data was performed using the two-tailed Student's t test.

Ex Vivo Viral Replication

$CD45^{100\%}$, $CD45^{62\%}$, or $CD45^{0\%}$ mouse splenocytes (1×10^6 cells/ml) were infected with a multiplicity of infection of 0.1 of mouse-adapted Ebola virus. Cell-free supernatants were harvested at 6, 24, 48, or 72 hr and were then subjected to traditional plaque assay for determination of viral titers.

Immunohistochemical Staining

To detect the presence of EBOV in infected organs, the tissue sections were deparaffinized, blocked in methanol-$HB_{2B}OB_{2B}$ solution for 30 min at room temperature (RT), rinsed with water, and pretreated with freshly diluted Proteinase K solution (20 μg/ml) for 15 min at RT. After blocking with the CAS block containing 5% goat serum, the sections were incubated with Rabbit anti-Ebola (994) antibody for 60 min at RT. After rinsing three times with PBS, peroxidase-labeled polymer conjugated to goat anti-rabbit immunoglobulins was added and incubated for 30 min. After rinsing with PBS, substrate-chromogen solution was added, incubated for 5 min, rinsed with PBS, stained with hematoxylin, and dehydrated, and tissues were mounted with Permount.

Apoptosis in tissues was detected by the TUNEL method using the Apoptag Plus peroxidase in situ apoptosis kit (Chemicon). Processing of the tissue samples was carried out as described above, with the following changes. After proteinase K treatment and washing, tissues were incubated with terminal deoxynucleotidyl transferase (TdT) for 60 min at 37°C. The reaction was stopped by adding stop/wash buffer and incubating for 10 min at RT. After washing three times with PBS, the tissues were incubated with anti-digoxigenin-peroxidase for 30 min at RT. Color development was visualized using the DAB substrate. Slides were counterstained with methyl green.

In Vivo Antibody Depletion

Lymphocyte subsets were depleted as described previously (Alici et al., 2007; King et al., 2008; Wang et al., 2003; Yang et al., 2006) by i.p. injection of 300 μg of functional grade antibodies on days −3, −1, and +3. Antibodies used to deplete lymphocyte subsets were NK1.1 (clone PK136), CD4 (clone GK1.5), CD8 (clone 53-6.7), CD90.2 (clone 30-H12), and a rat IgG1 isotype control, all purchased from eBioscience (San Diego, CA).

For the in vivo IFN-γ studies, 300 μg of functional grade anti-IFN-γ antibody (clone XMG1.2) or a rat IgG1 isotype control was injected i.p. on days −1, +1, +3, +6, and +11, similar to previously reported methods (Zhong et al., 2001).

Gene Expression Studies and Microarray Analysis

Splenocytes isolated from spleen of wild-type (100%) and/or heterozygous (62%) mice at days 0, 1, 3, 5, 7, 9, 11, and 13 were resuspended in 2 ml TRIzol solution. The samples were stored at −70°C until the RNA was purified. Total cellular RNA was isolated as per the manufacturer's specifications. The quality and concentration of the RNA were determined by measuring the absorbance at 260 and 280 nm. RNA integrity was confirmed using an Agilent 2100 Bioanalyzer (Agilent technologies, Palo Alto, CA). The mouse genome 430 2.0 array (Affymetrix, Inc.), which consists of more than 39,000 genes in a single array, was used. Affymetrix CEL files were preprocessed using *GCRMA* (version 2.12.1) (Wu et al., 2004) in R/Bioconductor (Gentleman et al., 2004) (http://www.bioconductor.org). Median $\log_2$ expression values within each sample type/time point with a coefficient of variation (CV) > 1.4 were chosen

using the Bioconductor package genefilter for agglomerative hierarchical clustering. Affymetrix control probesets, *Xist*, and genes on the Y chromosome were removed, and the probeset with the largest CV was chosen for genes with > 1 probeset. Cluster stability was assessed using the Bioconductor package clusterStab to suggest cluster boundaries. The probeset with the largest CV for each Entrez identifier was chosen for upload of median $\log_2$ ($CD45^{62\%}/CD45^{100\%}$ ratios) and EBarrays probabilities to Ingenuity Pathways Analysis version 6.3 (Ingenuity Systems, http://www.ingenuity.com). GO term enrichment was determined with the Bioconductor package GOstats (version 2.6.0) (Falcon and Gentleman, 2007) with annotation information from GO.db. Analyses were performed with a significance cutoff that posterior probability of no change < 1E − 10.

ACCESSION NUMBERS

Microarray data are available online at the Gene Expression Omnibus website (http://www.ncbi.nlm.nih.gov/geo), accession number XXX.

SUPPLEMENTAL DATA

Supplemental Data include one table and can be found with this article online at http://www.cell.com/cell-host-microbe/supplemental/S1931-3128(09)00248-0.

ACKNOWLEDGMENTS

We thank Christine Mech, Sean Van Tongeren, Jay Wells, and Meagan Cooper for technical support and Dr. Javad Aman for critical review of the manuscript. This project has been funded by the Defense Threat Reduction Agency (to R.G.P. and S.B.) and the National Institute for Allergy and Infectious Diseases (grant R43 A1055102 to W.C.R.). This project has been funded, in whole or in part, with federal funds from the National Cancer Institute, National Institutes of Health, under contract N01-CO-12400. The content of this publication does not necessarily reflect the views or policies of the Department of Health and Human Services, nor does mention of trade names, commercial products, or organizations imply endorsement by the U.S. Government. This research was supported, in part, by the Developmental Therapeutics Program in the Division of Cancer Treatment and Diagnosis of the National Cancer Institute. We would like to thank Oak Ridge Institute for Science and Engineering for participating in the Postgraduate Research Program at the U.S. Army Medical Research and Materiel Command. Opinions, interpretations, conclusions, and recommendations are those of the authors and are not necessarily endorsed by the U.S. Army.

Received: April 17, 2009
Revised: June 16, 2009
Accepted: July 14, 2009
Published: August 19, 2009

REFERENCES

Alexander, D.R. (2000). The CD45 tyrosine phosphatase: a positive and negative regulator of immune cell function. Semin. Immunol. *12*, 349–359.

Alici, E., Konstantinidis, K.V., Sutlu, T., Aints, A., Gahrton, G., Ljunggren, H.G., and Dilber, M.S. (2007). Anti-myeloma activity of endogenous and adoptively transferred activated natural killer cells in experimental multiple myeloma model. Exp. Hematol. *35*, 1839–1846.

Alonso, A., Sasin, J., Bottini, N., Friedberg, I., Friedberg, I., Osterman, A., Godzik, A., Hunter, T., Dixon, J., and Mustelin, T. (2004). Protein tyrosine phosphatases in the human genome. Cell *117*, 699–711.

Bowen, E.T., Platt, G.S., Simpson, D.I., McArdell, L.B., and Raymond, R.T. (1978). Ebola haemorrhagic fever: experimental infection of monkeys. Trans. R. Soc. Trop. Med. Hyg. *72*, 188–191.

Bradfute, S.B., Braun, D.R., Shamblin, J.D., Geisbert, J.B., Paragas, J., Garrison, A., Hensley, L.E., and Geisbert, T.W. (2007). Lymphocyte death in a mouse model of Ebola virus infection. J. Infect. Dis. *196* (*Suppl 2*), S296–S304.

Bradfute, S.B., Warfield, K.L., and Bavari, S. (2008). Functional CD8+ T Cell Responses in Lethal Ebola Virus Infection. J. Immunol. *180*, 4058–4066.

Bray, M., Davis, K., Geisbert, T., Schmaljohn, C., and Huggins, J. (1998). A mouse model for evaluation of prophylaxis and therapy of Ebola hemorrhagic fever. J. Infect. Dis. *178*, 651–661.

Byth, K.F., Conroy, L.A., Howlett, S., Smith, A.J., May, J., Alexander, D.R., and Holmes, N. (1996). CD45-null transgenic mice reveal a positive regulatory role for CD45 in early thymocyte development, in the selection of CD4+CD8+ thymocytes, and B cell maturation. J. Exp. Med. *183*, 1707–1718.

Connolly, B.M., Steele, K.E., Davis, K.J., Geisbert, T.W., Kell, W.M., Jaax, N.K., and Jahrling, P.B. (1999). Pathogenesis of experimental Ebola virus infection in guinea pigs. J. Infect. Dis. *179* (*Suppl 1*), S203–S217.

Couper, K.N., Blount, D.G., and Riley, E.M. (2008). IL-10: the master regulator of immunity to infection. J. Immunol. *180*, 5771–5777.

Desai, D.M., Sap, J., Silvennoinen, O., Schlessinger, J., and Weiss, A. (1994). The catalytic activity of the CD45 membrane-proximal phosphatase domain is required for TCR signaling and regulation. EMBO J. *13*, 4002–4010.

Falcon, S., and Gentleman, R. (2007). Using GOstats to test gene lists for GO term association. Bioinformatics *23*, 257–258.

Gentleman, R.C., Carey, V.J., Bates, D.M., Bolstad, B., Dettling, M., Dudoit, S., Ellis, B., Gautier, L., Ge, Y., Gentry, J., et al. (2004). Bioconductor: open software development for computational biology and bioinformatics. Genome Biol. *5*, R80.

Gibb, T.R., Bray, M., Geisbert, T.W., Steele, K.E., Kell, W.M., Davis, K.J., and Jaax, N.K. (2001). Pathogenesis of experimental Ebola Zaire virus infection in BALB/c mice. J. Comp. Pathol. *125*, 233–242.

Hermiston, M.L., Xu, Z., and Weiss, A. (2003). CD45: a critical regulator of signaling thresholds in immune cells. Annu. Rev. Immunol. *21*, 107–137.

Hoenen, T., Groseth, A., Falzarano, D., and Feldmann, H. (2006). Ebola virus: unravelling pathogenesis to combat a deadly disease. Trends Mol. Med. *12*, 206–215.

Hutchinson, K.L., and Rollin, P.E. (2007). Cytokine and chemokine expression in humans infected with Sudan Ebola virus. J. Infect. Dis. *196* (*Suppl 2*), S357–S363.

Irie-Sasaki, J., Sasaki, T., Matsumoto, W., Opavsky, A., Cheng, M., Welstead, G., Griffiths, E., Krawczyk, C., Richardson, C.D., Aitken, K., et al. (2001). CD45 is a JAK phosphatase and negatively regulates cytokine receptor signalling. Nature *409*, 349–354.

Kendziorski, C.M., Newton, M.A., Lan, H., and Gould, M.N. (2003). On parametric empirical Bayes methods for comparing multiple groups using replicated gene expression profiles. Stat. Med. *22*, 3899–3914.

Kim, M.O., Suh, H.S., Si, Q., Terman, B.I., and Lee, S.C. (2006). Anti-CD45RO Suppresses Human Immunodeficiency Virus Type 1 Replication in Microglia: Role of Hck Tyrosine Kinase and Implications for AIDS Dementia. J. Virol. *80*, 62–72.

King, S.B., Knorn, A.M., Ohnmacht, C., and Voehringer, D. (2008). Accumulation of effector CD4 T cells during type 2 immune responses is negatively regulated by Stat6. J. Immunol. *180*, 754–763.

McNeill, L., Salmond, R.J., Cooper, J.C., Carret, C.K., Cassady-Cain, R.L., Roche-Molina, M., Tandon, P., Holmes, N., and Alexander, D.R. (2007). The Differential Regulation of Lck Kinase Phosphorylation Sites by CD45 Is Critical for T Cell Receptor Signaling Responses. Immunity *27*, 425–437.

Moe, J.B., Lambert, R.D., and Lupton, H.W. (1981). Plaque assay for Ebola virus. J. Clin. Microbiol. *13*, 791–793.

Mohamadzadeh, M. (2009). Potential Factors Induced by Filoviruses that Lead to Immune Supression. Curr. Mol. Med. *9*, 174–185.

Mohamadzadeh, M., Chen, L., Olinger, G.G., Pratt, W.D., and Schmaljohn, A.L. (2006). Filoviruses and the balance of innate, adaptive, and inflammatory responses. Viral Immunol. *19*, 602–612.

Mohamadzadeh, M., Chen, L., and Schmaljohn, A.L. (2007). How Ebola and Marburg viruses battle the immune system. Nat. Rev. Immunol. *7*, 556–567.

Panchal, R.G., Ulrich, R.L., Bradfute, S.B., Lane, D., Ruthel, G., Kenny, T.A., Iversen, P.L., Anderson, A.O., Gussio, R., Raschke, W.C., et al. (2009).

Reduced expression of CD45 protein-tyrosine phosphatase provides protection against anthrax pathogenesis. J. Biol. Chem. *284*, 12874–12885.

Roach, T., Slater, S., Koval, M., White, L., Cahir McFarland, E.D., Okumura, M., Thomas, M., and Brown, E. (1997). CD45 regulates Src family member kinase activity associated with macrophage integrin-mediated adhesion. Curr. Biol. *7*, 408–417.

Ryabchikova, E., Kolesnikova, L., Smolina, M., Tkachev, V., Pereboeva, L., Baranova, S., Grazhdantseva, A., and Rassadkin, Y. (1996). Ebola virus infection in guinea pigs: presumable role of granulomatous inflammation in pathogenesis. Arch. Virol. *141*, 909–921.

Thomas, M.L. (1989). The leukocyte common antigen family. Annu. Rev. Immunol. *7*, 339–369.

Thomas, M.L., and Brown, E.J. (1999). Positive and negative regulation of Src-family membrane kinases by CD45. Immunol. Today *20*, 406–411.

Thomsen, A.R., Nansen, A., Madsen, A.N., Bartholdy, C., and Christensen, J.P. (2003). Regulation of T cell migration during viral infection: role of adhesion molecules and chemokines. Immunol. Lett. *85*, 119–127.

Towner, J.S., Sealy, T.K., Khristova, M.L., Albarino, C.G., Conlan, S., Reeder, S.A., Quan, P.L., Lipkin, W.I., Downing, R., Tappero, J.W., et al. (2008). Newly discovered ebola virus associated with hemorrhagic fever outbreak in Uganda. PLoS Pathog. *4*, e1000212.

Villinger, F., Rollin, P.E., Brar, S.S., Chikkala, N.F., Winter, J., Sundstrom, J.B., Zaki, S.R., Swanepoel, R., Ansari, A.A., and Peters, C.J. (1999). Markedly elevated levels of interferon (IFN)-gamma, IFN-alpha, interleukin (IL)-2, IL-10, and tumor necrosis factor-alpha associated with fatal Ebola virus infection. J. Infect. Dis. *179* (*Suppl 1*), S188–S191.

Virts, E.L., Diago, O., and Raschke, W.C. (2003). A CD45 minigene restores regulated isoform expression and immune function in CD45-deficient mice: therapeutic implications for human CD45-null severe combined immunodeficiency. Blood *101*, 849–855.

Virts, E.L., and Raschke, W.C. (2001). The role of intron sequences in high level expression from CD45 cDNA constructs. J. Biol. Chem. *276*, 19913–19920.

Wallace, V.A., Penninger, J.M., Kishihara, K., Timms, E., Shahinian, A., Pircher, H., Kundig, T.M., Ohashi, P.S., and Mak, T.W. (1997). Alterations in the level of CD45 surface expression affect the outcome of thymic selection. J. Immunol. *158*, 3205–3214.

Wang, G., Tschoi, M., Spolski, R., Lou, Y., Ozaki, K., Feng, C., Kim, G., Leonard, W.J., and Hwu, P. (2003). In vivo antitumor activity of interleukin 21 mediated by natural killer cells. Cancer Res. *63*, 9016–9022.

Warfield, K.L., Deal, E.M., and Bavari, S. (2009). Filovirus infections. J. Am. Vet. Med. Assoc. *234*, 1130–1139.

Warfield, K.L., Olinger, G., Deal, E.M., Swenson, D.L., Bailey, M., Negley, D.L., Hart, M.K., and Bavari, S. (2005). Induction of humoral and CD8+ T cell responses are required for protection against lethal Ebola virus infection. J. Immunol. *175*, 1184–1191.

Warfield, K.L., Swenson, D.L., Olinger, G.G., Nichols, D.K., Pratt, W.D., Blouch, R., Stein, D.A., Aman, M.J., Iversen, P.L., and Bavari, S. (2006). Gene-specific countermeasures against Ebola virus based on antisense phosphorodiamidate morpholino oligomers. PLoS Pathog. *2*, e1.

Wu, Z., Irizarry, R.A., Gentleman, R.C., Martinez-Murillo, F., and Spencer, F. (2004). A model-based background adjustment for oligonucleotide expression Arrays. J. Am. Stat. Assoc. *99*, 909–917.

Yang, Z., Day, Y.J., Toufektsian, M.C., Xu, Y., Ramos, S.I., Marshall, M.A., French, B.A., and Linden, J. (2006). Myocardial infarct-sparing effect of adenosine A2A receptor activation is due to its action on CD4+ T lymphocytes. Circulation *114*, 2056–2064.

Zamoyska, R. (2007). Why is there so much CD45 on T cells? Immunity *27*, 421–423.

Zhong, W., Roberts, A.D., and Woodland, D.L. (2001). Antibody-independent antiviral function of memory CD4+ T cells in vivo requires regulatory signals from CD8+ effector T cells. J. Immunol. *167*, 1379–1386.